

Irreversibility Fields in NbTi Superconducting Wires with Different Filament Diameters

Tsugio Hamada

National Institute of Technology, Miyakonojo College, Miyazaki 885-8567, Japan

Yusuke Hisamatsu

National Institute of Technology, Miyakonojo College, Miyazaki 885-8567, Japan

Hideki Noji

National Institute of Technology, Miyakonojo College, Miyazaki 885-8567, Japan

Abstract- The irreversibility fields in multifilamentary Nb-Ti wires were measured and were found to be seriously suppressed due to the flux creep at high temperatures while the critical current density was fairly large. This is explained by the small pinning potential as compared with a bulk specimen, since the pinning potential is limited by the size of filaments. The experimental results are compared to the prediction based on the flux creep theory. Quantitative difference exists in the vicinity of the critical temperature. This difference could be explained by the statistical method on the inhomogeneity in the specimens.

Keywords – Pinning Potential, Irreversibility Field, Superconductor, Nb-Ti Wire, Flux Bundle

I. INTRODUCTION

The irreversibility field of high temperature superconductor was suppressed seriously by the large thermal agitation of flux lines at high temperatures [1,2]. According to the flux creep theory [3], irreversibility field is governed by the magnitude of pinning potential. Recently, it was found that the irreversibility field of a thin film under a normal magnetic field was fairly smaller than that of a bulk specimen in spite of the larger critical current density. This result can be explained from the pinning potential. In this paper, we are going to explain the phenomenon by using a metallic superconductor that the pinning mechanism has been clarified. The pinning potential, V_b , is proportional to the flux bundle [4], given as

$$V_b = (ga_f)^2 l_{44} \quad (1)$$

for a bulk superconductor, where g^2 is the number of fluxoids inside the flux bundle, a_f is the fluxoids spacing, and l_{44} is the longitudinal correlation length of the fluxoids. If the size of superconductor, D , is smaller than l_{44} , V_b is limited by D and given by

$$V_b = (ga_f)^2 D \quad (2)$$

instead of Eq. (1). Similar limitation of the irreversibility field has been observed for multifilamentary wires with fine filaments even for a metallic superconductor. In this study, the irreversibility field in multifilamentary Nb-Ti wires is measured to investigate the validity of the description of the pinning potential in the collective flux creep theory for small superconductors.

II. EXPERIMENTS

Specimens investigated are Cu matrix Nb-47wt%Ti multifilamentary wires with fine filaments. The specifications of the specimens are listed in Table 1. The specimens were cut in units of 150 mm and were wound into a coil with a diameter of 7 mm. The magnetic field was applied normal to the wire up to 7 T. The critical current density, J_c , was estimated from the measurement of DC magnetization curve using the so called FC (Field Cooled) and ZFC

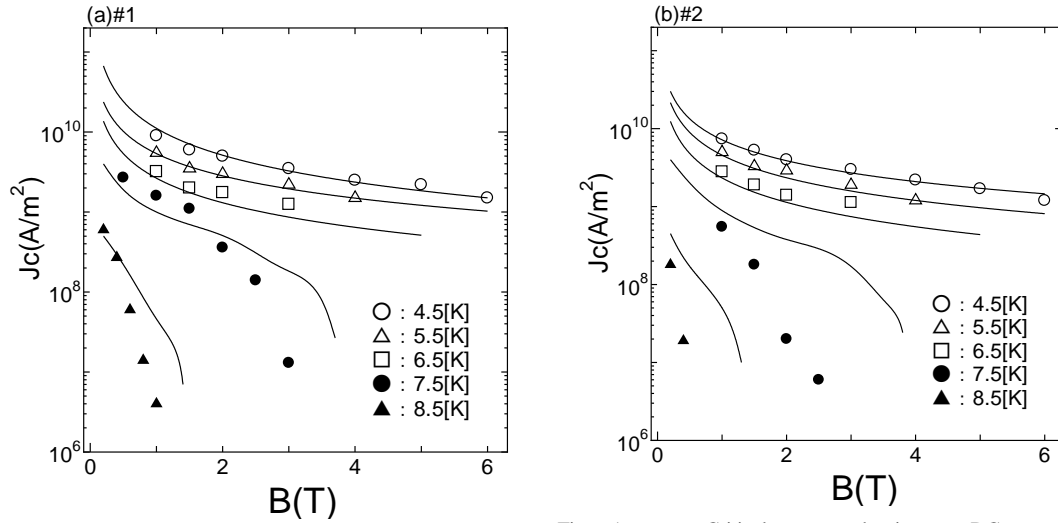


Figure 1. Critical current density vs. DC magnetic field of multifilamentary Nb-Ti wire specimens (a) #1 and (b) #2 at different temperatures. Solid lines show the virtual value given by Eq. (3) with the pinning parameters listed in Table 2.

(Zero Field Cooled) processes using a SQUID magnetometer. FC is a method to measure the magnetization for decreasing the temperature while applying a magnetic field to the superconductor. ZFC method is lowering the temperature of the superconductor in the magnetic field of zero. By comparing these two results, the magnetization value can be measured the irreversibility temperature. Inhomogeneity of the filament on the crosssectional surface is investigated by a SEM (scanning electron microscope) equipment.

III. EXPERIMENT AND RESULT

The critical current density, J_c , is estimated from the hysteresis of the magnetization, ΔM , in the formula, $J_c = 3\pi\Delta M/4d_f$ where d_f is the filament diameter. The results of the magnetic field, B , dependence of J_c of specimens #1 and #2 at difference temperatures are shown in Figs. 1. (a) and (b), respectively. The J_c value of #1 is larger than that of #2. The virtual critical current density, J_{c0} , in the flux creep-free case can be approximately obtained at low temperatures because the effect of thermal agitation is negligible. The J_{c0} is expressed by

$$J_{c0} = A[1 - (T/T_c)^2]^m B^{\gamma-1} [1 - \frac{B}{B_{c2}(T)}]^\delta \quad (3)$$

where A , m , γ , and δ are pinning parameters.

Specifications of the multifilamentary Nb-Ti wires used in this study are shown in Table 1. The multifilamentary Nb-Ti wire is generally developed for an application of using in a field of Alternating Current. For the design, Filament diameter, Filament spacing, and Twist pitch are important parameters. That is, electrical loss does not occur in a field of Direct Current in superconducting state. But, in the Alternating Current, a certain loss occurs in spite of the superconducting state. The loss can be decreased with considering the above parameters.

Table 1. Specifications of Nb-Ti specimens

Specimen no.		#1	#2
Wire diameter [mm]	D_w	0.144	0.300
Filament diameter [μm]	d_f	1.26	2.62
Filament spacing [μm]	d_N	0.31	0.64
Twist pitch [mm]	λ_t	1.46	5.35
The number of filaments	N_f	4152	4152
Critical temperature [K]	T_c	9.12	9.02

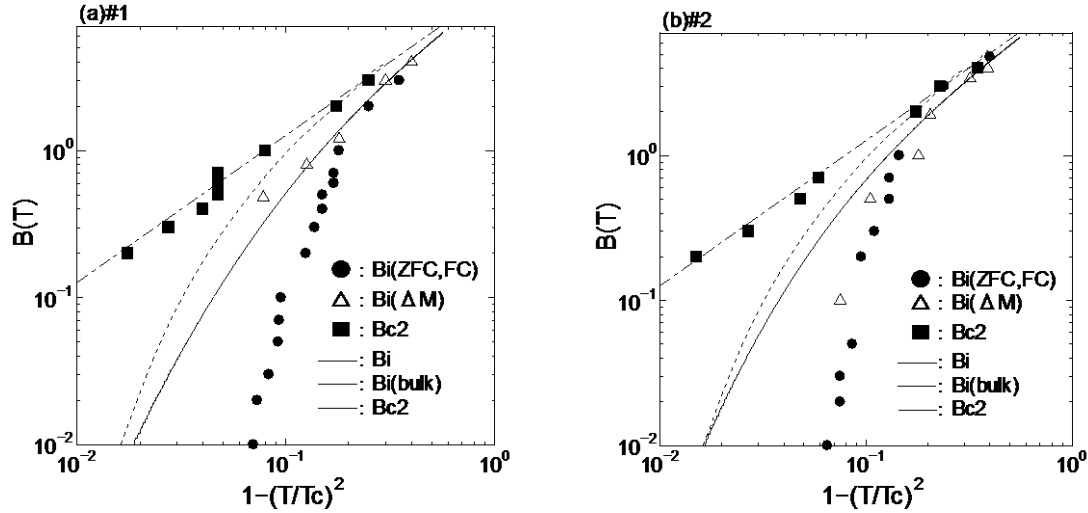


Figure2 Irreversibility field of specimens (a) #1 and (b) #2. Solid lines show the theoretical results corresponding to the measurement of B_i from ΔM .

The solid lines in Fig. 1 are determined so as to get a good agreement between Eq. (3) and experimental results at low temperatures ($T < 7.0$ K). The estimated pinning parameters are listed in Table 2. There seem to be as large as usually observed values.

The irreversibility field, B_i , and upper critical field, B_{c2} , are estimated from the measured results of FC (Field Cool) and ZFC (Zero Field Cool) processes.

Here we briefly explain how to estimate the B_i and B_{c2} . Fig.3 shows a schematic illustration of B - T plane in a superconductor. The B_i and B_{c2} have a dependence of temperature, respectively. The B_i is usually in the vicinity of the B_{c2} for the strongly pinned superconductors. The reversible region where the critical current density becomes zero despite of superconducting state exists between the B_{c2} and the B_i for the weakly pinned superconductors. Fig.4 shows a schematic illustration of the measurement of magnetization with changing the temperature and the magnetic field by the FC and ZFC processes. The applied magnetic field to the specimen for the decision of T_c is generally smaller than the lower critical magnetic field, B_{c1} . This is schematically shown the both ends arrow (ab) in Fig. 3. That is, the specimen not superconducting state is applied the magnetic field at room temperature, and is cooled to the liquid helium temperature in the case of FC process. The magnetic fields are through the specimen because the specimen is not superconducting state. When the specimen transits to the superconducting state at T_c , some fluxoids cannot move in order to be pinned. Therefore, the change of magnetization is not larger than that of the ZFC process in Fig.4. On the other hand, the magnetic field is applied to the specimen of superconducting state in the case of the ZFC process. Therefore, the fluxoids are not inside the specimen at low temperature. When temperature meets the T_c by increasing temperature, the fluxoids penetrate immediately into the specimen. Therefore, the large magnetization signal is observed in this case.

Let us consider the B_i and B_{c2} with comparing the Figs. 3, 4 and 5. In the case of cooling from room temperature along the both ends arrow (ab) in Fig. 3. The T_c to the applying magnetic field appears, and this magnetic field means the B_{c2} at this temperature. The fluxoids in the reversible region are moved by the Lorentz force, because the pinning forces do not acted to them. The fluxoids are pined when the cooling temperature attains the temperature of the irreversibility region. This temperature means the irreversibility temperature, T_i , and the strength of magnetic field is called as the B_i at this temperature. The magnitude of the magnetization below the temperature of the irreversible region is almost constant because the pinned fluxoids cannot move. Therefore, the reversible region in Fig.4 is decided between $T_c(B)$ and $T_i(B)$ against the certain magnetic field. Other $B_i(T)$ and $B_{c2}(T)$ can be decided in the same manner

Table 2 Pinning parameters defined in Eq. (3)

Specimen	A	$B_{c2}(0)[T]$	m	γ	δ
#1	1.7×10^{10}	12.5	2.19	0.50	1.0
#2	1.5×10^{10}	12.6	2.17	0.48	1.0

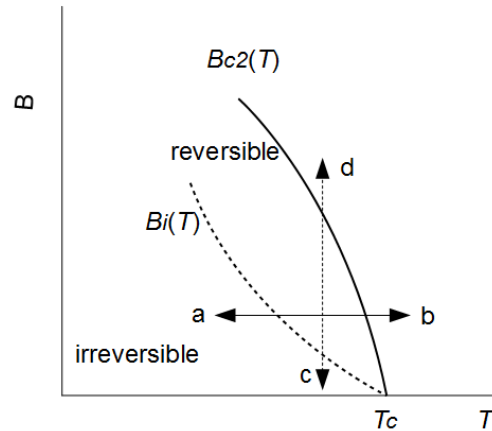


Figure 3. The reversible region where the critical current density becomes zero despite of superconducting state exists between the $B_{c2}(T)$ and the $B_i(T)$.

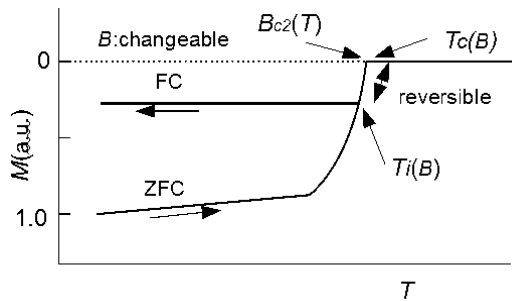


Figure 4. $B_i(T)$ and $B_{c2}(T)$ are decided by measuring the magnetization using FC and ZFC processes.

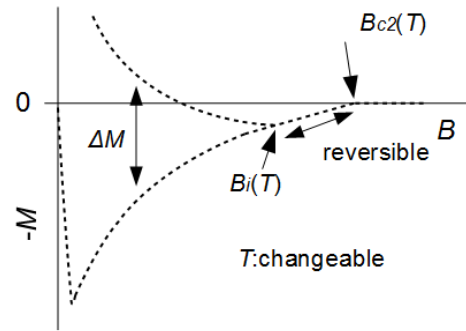


Figure 5. A schematic illustration of DC magnetization for weakly pinned superconductors.

using several magnetic fields. The $B_i(T)$ is also determined by the magnetic field at which the J_c obtained from the DC magnetization curve ΔM is equal to $\Delta J_c = 1.0 \times 10^7 \text{ Am}^{-2}$. However, the above mentioned ΔM is obtained from another DC magnetization measurement (see Fig.5). The schematic illustration of DC magnetization at certain temperature is shown in Fig.5. The processes of FC and ZFC changed the temperatures in a constant magnetic field. On the other hand, The DC magnetization measurement is changed the magnetic fields at a constant temperature. The $B_i(T)$ and $B_{c2}(T)$ are also decided as Fig.5. This is equivalent with the both ends arrow (cd) in Fig. 3. The results of B_i and B_{c2} of the two specimens are shown in Figs. 2 (a) and (b), respectively.

The open triangle symbol shows the result of B_i determined from ΔM . The difference between B_i and B_{c2} is small at low temperatures ($T < 7.0 \text{ K}$) and become large with increasing temperatures. The values of B_i determined from FC and ZFC magnetizations are comparable to those from ΔM for specimens #2 and is slightly larger than that from ΔM for specimens #1 in the range of $7.0 < T < 8.5 \text{ K}$. The difference between the B_i values from the two methods comes partially from the difference in the electric field which is lower for the measurement of FC and ZFC magnetizations, and hence, B_i from this method is more close to B_{c2} .

According to the flux creep theory in which the size of superconductor is taken into account [6], the pinning potentials are given by

$$U_0 = \frac{0.895 g^2 k_B J_{c0}^{1/2}}{\zeta^{3/2} B^{1/4}} \quad (l_{44} < d_f) \quad (4)$$

$$U_0 = \frac{4.23 g^2 k_B J_{c0} d_f}{\zeta B^{1/2}} \quad (l_{44} > d_f), \quad (5)$$

where k_B is the Boltzman constant, and behaves a role to connect energy with temperature. ζ is a constant depending on the kind of pinning center and $\zeta = 4$ is known for a strong and large pinning centers as αTi in the present case. In terms of U_0 , the condition of the irreversibility field is written as

$$U_0 \left(1 - \frac{\pi \Delta J_c}{2J_{c0}} \right) = k_B T \log \left(\frac{B a_f v}{E_c} \right), \quad (6)$$

where the sinusoidal washboard potential is assumed. v is the oscillation frequency of flux bundle and E_c is the electric field criterion for determination of J_c . From Eq. (4)-(6), we get the following two equations for the irreversibility field.

$$\frac{0.835 g^2 J_{c0}^{1/2}}{\zeta^{3/2} T} \left(1 - \frac{\pi \Delta J_c}{2J_{c0}} \right) = B^{1/4} \log \left(\frac{B a_f v}{E_c} \right) \quad (l_{44} < d_f) \quad (7)$$

$$\frac{4.23 g^2 J_{c0} d_f}{\xi T} \left(1 - \frac{\pi \Delta J_c}{2J_{c0}} \right) = B^{1/2} \log \left(\frac{B a_f v}{E_c} \right) \quad (l_{44} > d_f) \quad (8)$$

The calculated results of B_i from ΔM are shown by solid lines in Fig. 2, where the theoretically obtained $g^2 = 1$ is used in present region and $E_c = 10^{-10} \text{Vm}^{-1}$ is assumed. Within the range of FC and ZFC are slightly closer to B_{c2} compared to the results of B_i from ΔM due to the more strict criterions of E_c and ΔJ_c . These are not plotted in Fig. 2. For comparison, the broken lines show the results for a bulk specimens, where $d_f > l_{44}$. It is found that the bulk value of B_i is closer to B_{c2} . It was reported that B_i of a bulk Pb-Bi specimen was close to B_{c2} in spite of the low critical current density. Thus, the smaller irreversibility field in multifilamentary wires is due to the restriction of the volume of the flux bundle by the collective flux creep theory. However, the theoretical result of B_i is fairly larger than the experimental result in the vicinity of T_c . This may be explained from the spatial inhomogeneity of the superconductor such as the critical temperature, the filament diameter and the flux pinning strength.

The influence of inhomogeneity for the pinning strength was studied by Hamada et al [5]. If we assume a sinusoidal washboard potential, the dependence of the activation energy on the current density $U(j)$ is express as

$$U(j) = U_0 \left[(1 - j^2)^{\frac{1}{2}} - j \cos^{-1} j \right], \quad (9)$$

where j is the current density normalized by the virtual critical current density in the creep-free case, J_{c0} . An electric field is induced even in the pinned state below the flux flow region by the thermally activated motion of fluxoids. According to the one-dimensional flux creep model, it is given by

$$E_{cr} = B a_f v \left[\exp \left(\frac{-U(j)}{k_B T} \right) - \exp \left(\frac{-U'(j)}{k_B T} \right) \right] \quad (10)$$

where U and U' are the activation energies for fluxoids motion forwards and backwards, respectively, in relation to the direction of the Lorenz force. Then Eq. (10) is written as

$$\begin{aligned} E_{cr} &= B a_f v \times \exp \left[\frac{-U(j)}{k_B T} \right] \times \left[1 - \exp \left(\frac{-\pi U(j)}{k_B T} \right) \right] \quad (1 < j) \\ E_{cr} &= B a_f v \times \left[1 - \exp \left(\frac{-\pi U(j)}{k_B T} \right) \right] \quad (1 > j) \end{aligned} \quad (11)$$

,where $v = \rho_f J_{c0} / a_f B$ is calculated, and ρ_f is the flux flow resistivity, for which the Bardeen-Stephen model is assumed $\rho_f = (B/B_{c2}) \rho_n$. On the other hand, the contribution from the flux flow, E_{ff} , is given by

$$\begin{aligned} E_{ff} &= 0 \quad (1 > j) \\ &= \rho_f (j - J_{c0}) \quad (1 < j). \end{aligned} \quad (12)$$

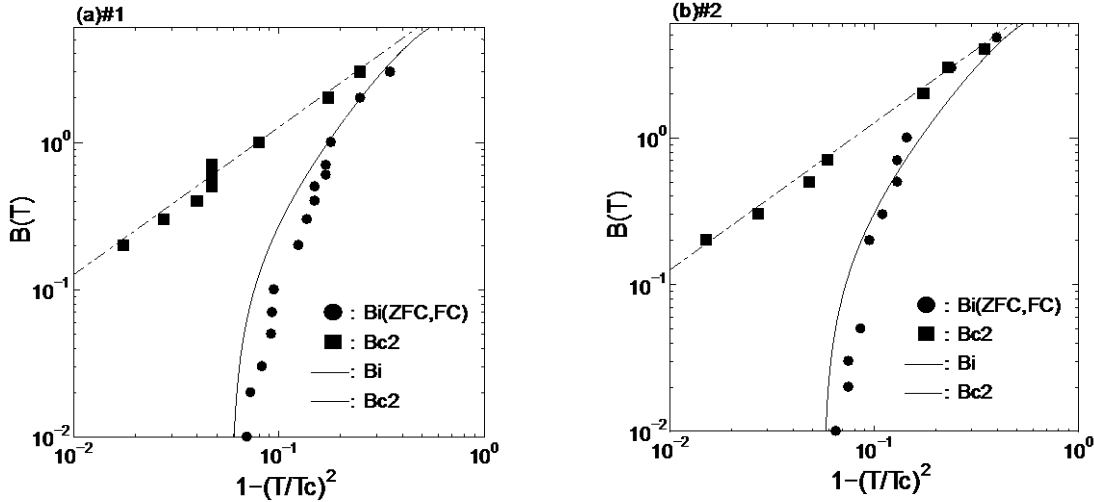


Figure 6. The theoretically calculated irreversibility fields of specimens (a) #1 and (b) #2. They fit in the vicinity of the filament diameter as opposed to the results showed in Fig. 2.

Here we assume that the total electric field is simply given by $E = E_{cr} + E_{ff}$, where E_{cr} is the electric field by the flux creep.

From here, we consider an influence of distribution of the filament diameter. The ununiformity of the filament diameters in the cross-sectional surface is investigated by a SEM equipment. From the obtained SEM images, the standard deviations are estimated using a statistical method. The values obtained are listed in Table 3. We assume

$$f(d_f) = \frac{K}{\sqrt{2\pi}\sigma} \exp\left[-\frac{(d_f - d_{f0})^2}{2\sigma^2}\right] \quad (13)$$

We assume that the distribution of filament diameters is shown in the Gaussian distribution. Since d_f should be positive, d_{f0} is approximately the mean value. K is approximately use $K = 1$.

The virtual critical current density, J_{c0} , which is shown in Eq.(3) is reconsidered to introduce a distribution of the filament diameter. In this study, we assume the size of the filament diameter, to affect the performance of the superconductor, J_{c0} value as written

$$J_{c0} = A^* [1 - (T/T_c)^2]^m B^{\gamma-1} (1 - B/B_{c2}(T))^{\delta} \quad (14)$$

We assume that only A depends on d_f . When d_f is smaller than d_{f0} , the filament has decreased performance of the superconductor because it's snapped. When d_f is bigger than d_{f0} , filaments are adjoin each other and become the lump. With the lump of the filament, the performance as the superconductor decreases. Thus, we have

$$\begin{aligned} A^* &= A(d_f/d_{f0})^6 & (d_f < d_{f0}) \\ &= A(d_{f0}/d_f)^6 & (d_f > d_{f0}) \end{aligned} \quad (15)$$

where A is a constant. As a result, the electric field is calculated by

$$E = (E_{cr} + E_{ff})f(d_f)d_f \quad (16)$$

The calculated results are shown in Figs. 6(a) and (b), respectively. It is found that the calculated line in Fig.6 fit generally to the experimental data. The statistical parameters used in this calculation are listed in Table 3. The cross sectional surface of the wires are observed and measured the diameter of some filaments by a SEM equipment. The mean value and the standard deviation of the filament diameters are obtained from the SEM images using the statistical estimation method. The calculation results are close to the experimental ones. This means the filament diameters of the wires have an ununiformity in the two-dimensional area.

Table 3 Statistical parameters for using in the calculation

Specimen	σ	$d_{f0} [\mu m]$
#1	0.30×10^{-6}	1.26
#2	0.62×10^{-6}	2.62

For more study, if we use the statistical parameters considered with longitudinal distribution of the filaments using the statistical estimation method, the calculation results will fit better with the experimental results. It is important for fabrication of the high quality multifilamentary wires to develop production technics and equipment so as to reduce the ununiformity of the filament diameters.

IV. CONCLUSION

The irreversibility field in multifilamentary Nb-Ti wire were measured and compared with the result of the flux creep theory. Following results are obtained.

(1) The irreversibility fields are remarkably suppressed due to the limitation of the filament size. Namely, the pinning potential is determined by the filament size when the longitudinal correlation length is larger than the filament size.

(2) The temperature dependence of the irreversibility field is approximately explained by the flux creep theory. However, the quantitative dependence of the irreversibility fields for the experimental data and theoretical data are explained by considering the distribution of filament diameter size.

REFERENCES

- [1] T. Matsushita and N. Ihara, "Scaling Current-Voltage Characteristics in High Temperature Superconductor", *Proc. 7th Int. Workshop on Critical Currents in Super-conductors*, pp. 169-173, 1994.
- [2] T. Matsushita., T. Tohdoh and N. Ihara, "Effects of inhomogeneous flux pinning strength and flux flow on scaling of current-voltage characteristics in high-temperature superconductors", *Physica C*, vol. 259, pp. 321-326, 1996
- [3] T. Matsushita and N. Ihara, "Flux Pinning Characteristics of Y-Ba-Cu-O in the Vicinity of Irreversibility Line", *Proceedings of the 6th International Symposium on Superconductivity in Japan*, pp. 507-510, 1993.
- [4] E.S.Otobe, T. Matsushita, T. Nakatani., N. Ihara, K. Noda, T. Umemura, M. Waka, M. and F. Uchikawa "IRREVERSIBILITY LINES IN Bi-2212 SUPER-CONDUCTORS", *Proceedings of the 6th International Symposium on Superconductivity in Japan*, pp.499-502. 1993
- [5] T. Hamada, T. Matsushita, B. Ni, T. Akune. and N. Sakamoto, "Change of irreversibility fields in pinning-strength-controlled metallics uperconductors", *Supercond. Sci. Technol.*, vol. 9, pp. 574-577, 1996.